

Adding a Computationally-Tractable Probabilistic Dimension to Meta-Heuristic-Based Microgrid Sizing

Soheil Mohseni, Alan C Brent,
Daniel Burmester, Will N Browne

Sustainable Energy Systems, Wellington Faculty of
Engineering, Victoria University of Wellington
Wellington, 6140, New Zealand

Scott Kelly

Institute for Sustainable Futures
University of Technology Sydney
Sydney, NSW, 2007, Australia

Abstract—A robust solution to the optimal micro-grid (MG) sizing problem requires comprehensive quantification of the underlying parametric uncertainties – particularly, the uncertainty in forecasts of meteorological, load demand, and wholesale electricity price time-series data. However, the associated data-driven processes for probabilistic uncertainty quantification are computationally expensive. Accordingly, the mainstream meta-heuristic-based MG sizing literature has failed to concurrently quantify more than four sources of forecast uncertainty. To address this knowledge gap, this paper introduces a novel computationally efficient, probabilistic MG sizing model that enables the simultaneous treatment of any (reasonable) number of data uncertainty. This provides a platform to characterize the uncertainty in ambient temperature and river streamflow for the first time in the MG optimal sizing literature. Importantly, the model supports the associated long-term strategic MG energy planning optimization processes through in-depth analyses of the worst-case, most likely case, and best-case planning scenarios. To demonstrate the utility of the proposed model for community MG projects, a case study is presented for the town of Ohakune, New Zealand. Notably, the numeric simulation results have shown that the whole-life cost of the conceptualized MG would have been underestimated and overestimated by as much as ~17% and ~30% respectively in the best-case and worst-case scenarios if the problem-inherent uncertainties were not explicitly factored into the associated techno-economic analyses.

Index Terms—Forecast uncertainty, Microgrids, Optimization, Power system planning, Probabilistic computing.

I. INTRODUCTION

The optimal sizing and designing of a micro-grid (MG) aims to minimize the whole-life cost of installing new distributed generation and storage technologies and the associated power conversion apparatuses, as well as the cost of purchasing energy from the grid (where applicable), over the analysis period, whilst adhering to a set of operational- and planning-level constraints [1]. To this end, the standard MG capacity planning problem conducts an hourly-resolved, year-long energy management analysis for each candidate mix of the size of the components, which makes the problem computationally intensive [2]. On the other hand, the

underlying energy scheduling problems that need to be solved as part of the aforementioned energy management analyses deal with various stochastic input parameters, such as forecasts of power loads, weather conditions, and wholesale electricity market prices (in grid-connected systems). Such sources of data uncertainty affect the energy management analyses, and the associated errors potentially propagate upward into the outer optimal MG sizing problem [3]. Accordingly, a recent, growing body of literature has formulated a range of stochastic MG sizing models, the associated solution algorithms of which can be broadly categorized into two classes [4]: (1) analytical (exact mathematical) solution algorithms, and (2) meta-heuristic optimization-based solution algorithms.

As notable instances of the analytically solved probabilistic MG sizing models, mixed-integer linear programming (MILP)- and mixed-integer nonlinear programming (MINLP)-based renewable energy system capacity planning models are developed in [5], [6]. Although these approaches do not generally suffer from any computational complexity issues, they are associated with several simplifications to decompose the outer investment planning and inner operational planning decision-making processes. Accordingly, the accuracy of these methods depends primarily on the efficiency of the underlying decomposition techniques, as well as the associated mean-field and (non)linear relaxation approximations. However, the actual accuracy of exact mathematical solution approaches has not been evaluated in practically all the analytical models available in the literature as this requires knowledge of the truly optimal solution. On the other hand, swarm-based meta-heuristic optimization algorithms do not require any mathematical model approximations. However, when the number of decision variables grows, the running time for meta-heuristic-based solution approaches soon becomes prohibitively large. Such limiting factors are more prominent for data-driven stochastic solution algorithms where the number of the associated function calls and fitness evaluations is significantly larger than the corresponding deterministic methods – which result in significantly increased computational execution times.

In this light, although their potential outperformance has been statistically validated in various MG capacity planning

studies [7], the existing meta-heuristic-based methods have failed to simultaneously address multiple problem-inherent forecast uncertainties. Table I summarizes the most notable meta-heuristic-based MG sizing approaches that have attempted to characterize at least one source of data uncertainty.

TABLE I. SUMMARY OF STOCHASTIC META-HEURISTIC-BASED STUDIES

Reference	Meta-heuristic optimizer	Uncertain Parameters(s)
[8]	Particle swarm optimization (PSO)	Load demand
[9]	PSO	Irradiance, load demand
[10]	Accelerated PSO	Irradiance, load demand
[11]	Binary PSO	Wind speed, irradiance, load
[12]	Weighted improved PSO	Wind speed, irradiance
[13]	Genetic algorithm	Irradiance, load, spot prices
[14]	Genetic algorithm	Irradiance, load demand

From the literature review emerge a number of key knowledge gaps, namely: (1) intractability of the existing meta-heuristic-based approaches to simultaneously quantify more than three sources of parametric uncertainty, (2) negligence of the uncertainty coupled with ambient temperature and river streamflow (for potential micro-hydropower), and (3) lack of attention to fundamentally new meta-heuristics. In response, this paper introduces a comprehensive, robust, general MG designing and capacity planning optimization model able to address multiple parametric uncertainties – solar irradiance, ambient temperature, wind speed, electricity price, load demand, and river streamflow forecasts – at a time, based on a state-of-the-art meta-heuristic. A key contribution of the paper is integrating a heuristic, MILP-based scenario reduction algorithm as part of the innovative new energy planning optimization model for community MGs, which facilitates the characterization of any (reasonable) number of data uncertainties during the associated investment planning decision-making processes that are aware of the corresponding aggregate uncertainty budgets.

II. TEST-CASE SYSTEM

A grid-tied community MG system integrating solar photovoltaic (PV) panels, wind turbines (WTs), a run-of-the-river micro-hydro power plant (MHPP), and a Li-ion battery bank is considered as a test case, as shown in Fig. 1.

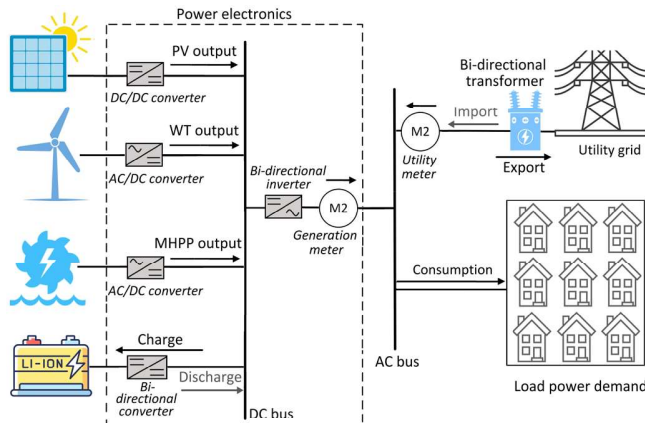


Figure 1. Schematic of the grid-tied, DC-linked community test-case MG.

A. PV Panels

The power output from each PV panel at time-step t is [15]:

$$P_{PV}(t) = \eta_{PV}(t) \cdot a_{PV} \cdot I_G(t), \quad (1)$$

$$\eta_{PV}(t) = \eta_r + (1 - \beta(T_c(t) - T_{c,ref})), \quad (2)$$

$$T_c(t) = T_a(t) + \left(\frac{NOCT - 20}{0.8} \right) I_G(t), \quad (3)$$

where $\eta_{PV}(t)$ denotes the panel's efficiency at time-step t , a_{PV} is the area of the panel (1.64 m^2), I_G represents solar irradiance [kW/m^2], η_r denotes the panel's rated efficiency (17.4%), β denotes the PV temperature coefficient of power ($-0.48\%/^\circ\text{C}$), T_c denotes the cell temperature, $T_{c,ref}$ denotes the reference cell temperature (25°C), T_a denotes the ambient temperature [$^\circ\text{C}$], and $NOCT$ denotes the nominal operating cell temperature (43°C).

B. Wind Turbines

The power output from each WT at time-step t can be obtained from [15]:

$$P_{WT}(t) = \begin{cases} 0 & \text{if } v(t) \leq v_{ci} \text{ or } v(t) \geq v_{co}, \\ A & \text{if } v_{ci} < v(t) \leq v_r, \\ P_{WT,r} & \text{if } v_r < v(t) < v_{co}, \end{cases} \quad (4)$$

$$A = \frac{P_{WT,r}}{v_r^3 - v_{ci}^3} v^3(t) - \frac{v_{ci}^3}{v_r^3 - v_{ci}^3} P_{WT,r}, \quad (5)$$

where $v(t)$ is wind speed at time-step t , v_{ci} , v_{co} , and v_r respectively denote the WT's cut-in wind speed (3.5 m/s), cut-out wind speed (25 m/s), and rated wind speed (14 m/s), while $P_{WT,r}$ represents the WT's rated power (225 kW).

C. Micro-Hydro Power Plant

The power output from each micro-hydro turbine at time-step t can be calculated by the following equation [15]:

$$P_{MH}(t) = P_{MH,r} \cdot \eta_{MH} \cdot \rho \cdot g \cdot h_g \cdot F(t), \quad (6)$$

where $P_{MH,r}$ denotes the micro-hydro turbine's rated power (100 kW), η_{MH} is the micro-hydro turbine's efficiency (78%), ρ denotes the water density (1000 kg/m^3), g is the gravity acceleration (9.81 m/s^2), h_g denotes the static (gross) head (10 m), and $F(t)$ is river streamflow at time-step t [m^3/s].

D. Battery Bank

The overall battery bank is modelled by its time-variant energy in-store level, as follows [15]:

$$E(t) = E(t-1)(1 - \sigma \cdot \Delta t) + P_{ch}(t) \cdot \eta_{ch} \cdot \Delta t - \frac{P_{dch}(t) \cdot \Delta t}{\eta_{dch}}, \quad (7)$$

where σ is each battery pack's self-discharge rate (0.3%/day), $P_{ch}(t)$ and $P_{dch}(t)$ respectively denote the charging power and discharging power at time-step t [kW], η_{ch} and η_{dch} respectively denote the charge and discharge efficiencies (97.5%), while Δt represents the length of each time-step (1 h).

E. Transformer and Power Conditioning Devices

The bi-directional transformer is modelled by a constant efficiency (93%), while the power factor is assumed to be 95%. Also, except for the bi-directional (multi-mode) inverter, the costs and efficiencies of the power electronics devices are reflected in the components they link to the DC bus. The bi-directional inverter's efficiency is assumed to be 98.5%.

F. Operational Strategy

The rule-based cycle-charging energy scheduling strategy, which seeks to maximize the grid-tied MG's self-sufficiency is chosen to decide the dispatch of the system [16]. Under the cycle-charging strategy, the onsite non-dispatchable renewable generation is first supplied to local loads with any excess power charging the storage devices before being fed back into the wider utility network. Also, any positive net load (local load minus onsite non-dispatchable generation) is served by discharging the storage first before importing from the grid.

III. STOCHASTIC MG SIZING MODEL

This section formulates the developed meta-heuristic-based stochastic MG sizing model that systematically quantifies any (reasonable) number of forecast uncertainties during the MG designing and capacity planning processes. In line with the secondary contributions of the paper, namely characterizing the uncertainty associated with river streamflow and ambient temperature forecasts – in conjunction with treating the uncertainty in solar irradiance, wind speed, load demand, and wholesale prices – the model is specifically parametrized for the conceptual test-case system. However, it can be readily adapted for application to any on- and off-grid MG configuration – and characterize any set of uncertain factors desired during the long-term MG investment planning phase.

A. Objective Function

The objective function seeks to minimize the total net present cost (NPC) of the modelled MG system, as follows:

$$\min TNPC = \sum_{c \in C} NPC(c) + NPC(P_{im} \cdot \pi_{ws} - P_{ex} \cdot FiT). \quad (8)$$

In (8), the term $NPC(c)$ denotes the net present cost of component c , the term $NPC(P_{im} \cdot \pi_{ws} - P_{ex} \cdot FiT)$ denotes the total net cost of energy exchanges with the grid over the MG lifespan in the present value, P_{im} and P_{ex} are the importing power and exporting power, respectively, with π_{ws} and FiT respectively denoting the variable wholesale price and fixed feed-in-tariff. The NPC of each component incorporates the capital cost, the present value replacement and operation and maintenance costs, as well as the present salvage value.

B. Constraints

For a technically robust optimal solution, the objective function needs to adhere to a set of constraints, as [17], [18]:

$$E_B(0) = 0.5N_B \cdot C_{B,r}, \quad (9)$$

$$E_B(T) \geq E_B(0), \quad (10)$$

$$LPSP \leq LPSP^{max}, \quad (11)$$

$$SSR \geq SSR^{min}, \quad (12)$$

$$0 \leq N_c \leq N_c^{max}, \quad (13)$$

$$0 \leq P_{im}(t) \leq N_{T,r} \cdot P_{T,r}, \quad (14)$$

$$0 \leq P_{ex}(t) \leq N_{T,r} \cdot P_{T,r}. \quad (15)$$

To cost-efficiently handle the peaks that occur early in the time-series load data, (9) sets the battery bank's initial state-of-charge (SOC) to be half-full-charged as determined by multiplying the optimal number of battery packs, N_B , which is obtained over the course of iterations, by the nameplate capacity of each battery pack, $C_{B,r}$, divided by 2. Eq. (10) ensures that the battery bank's terminal SOC (at the last

iteration) equals or exceeds its initial (pre-set) SOC for a balanced analysis. A specifically formulated maximum loss of power supply probability index, $LPSP^{max}$, and a minimum self-sufficiency ratio, SSR^{min} , are relaxed using (11) and (12), respectively. Also, lower and upper limits are placed on the optimal size of the equipment in (13), while the energy trading with the wider network is enforced to adhere to the bi-directional transformer's capacity in (14) and (15).

C. Meta-Heuristic Optimization Algorithm

The moth-flame optimization algorithm (MFOA) [19] is used in the solution algorithm as it has been demonstrated to be a comparatively computationally efficient algorithm, and superior to a broad spectrum of both well-established and state-of-the-art meta-heuristics in terms of nearing the globally optimum solutions in the long-term strategic MG planning applications [1], [2], [7], [15], [20], [21]. The MFOA, which is inspired by the navigation mechanism of moths at night, can be expressed mathematically as [19]:

$$M_i = S(M_i, F_j), \quad (16)$$

$$S(M_i, F_j) = |F_j - M_i| \cdot e^{bt} \cdot \cos(2\pi r) + F_j, \quad (17)$$

where $S(M_i, F_j)$ denotes a logarithmic spiral function of the positions of moths (M_i) and flames (F_j), b is a constant that defines the shape of the spiral (here, $b = 1$), r is a pseudo-random number in the range $[-1, 1]$, and $|F_j - M_i|$ is the Euclidean distance between the i -th moth and the j -th flame.

D. Probabilistic Uncertainty Characterization

A probabilistic dimension is added to the above-described deterministic MG sizing model by the following steps:

1) *PDF Construction*: The best-fitting distributions of the associated historical data for the corresponding random variables (uncertain inputs) are utilized to derive the hourly probability distribution functions (PDFs). Specifically, the beta, Weibull, and gamma distributions are used to model the variability inherent in solar irradiance, wind speed, and river streamflow data streams, respectively. The wholesale electricity market price, power loads, and ambient temperature datasets are assumed to be normally distributed.

The PDF of the beta distribution to model the behavior of the random variable $0 \leq x \leq 1$ with shape parameters $\alpha, \beta > 0$ can be expressed as follows:

$$f(x) = \frac{\Gamma(\alpha + \beta)}{\Gamma(\alpha)\Gamma(\beta)} x^{\alpha-1} (1-x)^{\beta-1}. \quad (18)$$

The PDF of a Weibull random variable $x \geq 0$ with a shape parameter $k > 0$ and a scale parameter $c > 0$ is given by:

$$f(x) = \frac{k}{c} \left(\frac{x}{c}\right)^{k-1} e^{-\left(\frac{x}{c}\right)^k}. \quad (19)$$

The PDF of the gamma distribution for variable $x > 0$ with a shape parameter α and a rate parameter β is:

$$f(x) = \frac{\beta^\alpha x^{\alpha-1} e^{-\beta x}}{\Gamma(\alpha)}. \quad (20)$$

The PDF of a normally distributed variable x with mean μ and standard deviation σ can be expressed as follows:

$$f(x) = \frac{1}{\sqrt{2\pi}\sigma} e^{-\frac{1}{2}\left(\frac{x-\mu}{\sigma}\right)^2}. \quad (21)$$

2) *PDF Discretization*: The hourly uncertain parameter-specific PDFs are then discretized into equal-width regions. More specifically, the equal-width regions divide the corresponding range of possible values into a set of mutually exclusive and collectively exhaustive intervals. The arithmetic means and the associated probabilities of occurrence of the resulting intervals are then determined to represent the equal-width regions in the following scenario generation processes. Accordingly, the accuracy of the associated approximations depends primarily on the granularity step size for PDF discretization.

The preliminary benchmark tests revealed that approximating the continuous PDFs by seven equal-width regions offers the best compromise between solution quality and computational intensity.

3) *Scenario Vector Generation*: A set of $7^6 = 117,649$ scenario vectors were generated for each hour of the MG operation in accordance with all possible combinations of the six uncertain inputs represented by seven equal segments of the associated PDFs.

4) *Scenario Vector Reduction*: To alleviate the computational burden, the scenario vectors were then clustered to seven for each hour of the MG operation using a MILP-based scenario reduction algorithm [22]. The algorithm guarantees that the overall probability of a particular realisation of each uncertain parameter at time-step t in the final scenario set is equal to the probability of the uncertain parameter taking on that value. It has been demonstrated that the scenario reduction algorithm's efficacy in representing the original scenarios lies in the 0.5% to 2% range [22]. The validity of this claim in the stochastic MG planning applications has been statistically verified based on a number of small-scale benchmark probabilistic MG sizing case studies.

5) *Model Evaluation*: The deterministic model is then solved for each reduced scenario vector, and the modelling results, as well as the corresponding posterior probabilities of the multi-dimensional scenarios, are recorded.

6) *Outcome Analysis*: Finally, the cumulative normal distributions that provide the best fit to the output histograms are produced in accordance with the posterior probabilities assigned by the scenario reduction algorithm. Then, to provide tailored support to the associated MG planning decision-making processes – and designing cost-efficient MGs under different uncertainty budgets – the expected values, as well as the 5th and 95th percentiles of the cumulative distributions of the model outputs, are determined, which respectively represent the most likely, best-case, and worst-case projection energy planning scenarios.

E. Overview of the Model

Fig. 2 illustrates the structure of the meta-heuristic-based solution algorithm for the proposed stochastic MG capacity optimization model.

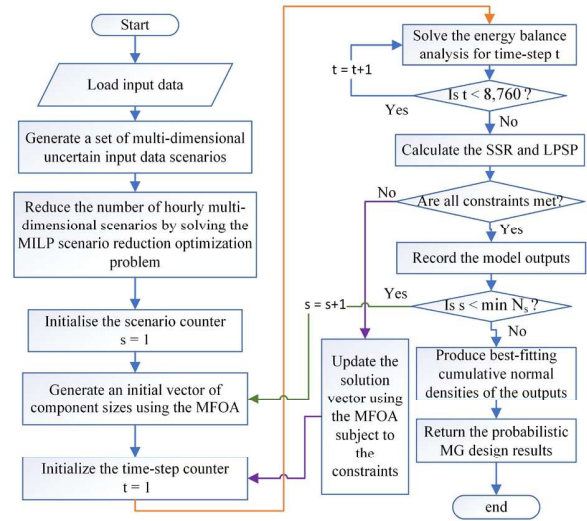


Figure 2. Meta-heuristic-based probabilistic MG sizing solution algorithm.

IV. INPUT DATA: THE CASE OF OHAKUNE, NEW ZEALAND

The developed model was populated for the case of the town of Ohakune (latitude 39.4180°S, longitude 175.3985°E) to provide a reliable, affordable, sustainable local electricity generation solution that addresses the existing transmission congestion issues [23]. Located in the center of New Zealand's North Island, the town has a permanent population of around 1,200 people, according to the most recent census (Stats New Zealand, 2018). The permanent population of the town live in detached and semi-detached houses, and the most dominant household size is 2 persons according to the census. Table II summarizes the techno-economic specifications of the selected product models of the generation, storage, and conversion technologies for implementation in Ohakune. The associated main components are available off the shelf; they were chosen based on the primary author's experience – on the trade-off between technical performance and economic viability – from the options available in the New Zealand and Australian renewable energy asset markets. In this paper, costs are always cited in 2019 NZ\$ (the 2019 annual average exchange rate: NZ\$1 = US\$0.69). Also, the project lifespan and real interest rate were respectively assumed to be 20 years and 3.7%.

TABLE II. TECHNO-ECONOMIC SPECIFICATIONS OF THE EQUIPMENT

Component	Capital cost	Replacement cost	O&M cost	Lifetime
PV panel	\$1,135/kW	N/A	\$4.2/kW/yr	20 years
WT	\$1,290/kW	N/A	\$21/kW/yr	20 years
MHPP	\$840/kW	N/A	\$15/kW/yr	20 years
Battery	\$901/kWh	\$553/kWh	\$5.5/kWh/yr	15 years
Inverter	\$760/kW	\$580/kW	\$1.1/kW/yr	15 years
Transformer	\$65/kVA	N/A	\$0.3/kVA/yr	20 years

The historical meteorological data are based on 10 years' (2010 to 2019) worth of data retrieved from the New Zealand's National Institute of Water and Atmospheric Research's 'CliFLO' database [24] with an hourly resolution. The hourly-resolved, year-long load demand data were specifically synthesized based on the findings of the New Zealand GREEN grid household electricity demand study [25], in accordance with the town's household size distribution.

To achieve the statistical representativeness necessary to ensure the quality of the associated PDF generation process, the synthetic power data stream was then augmented using an unreported Markov chain model. Specifically, the derived power load dataset was regenerated 9 times. Furthermore, the 10-year (2010 to 2019) historical locational marginal price data were retrieved from the New Zealand's Electricity Market database [26]. Moreover, the feed-in-tariff was considered to be \$0.08/kWh.

V. SIMULATION RESULTS AND DISCUSSION

This section presents the simulation results. The developed model was coded in MATLAB and executed on a desktop computer with a Core i7 3.20 GHz CPU and 16 GB RAM. As an example of the hourly input scenario vectors, Table III presents the posterior probabilities of the reduced multi-dimensional scenarios obtained by solving the MILP scenario reduction algorithm – using the built-in ‘*intlinprog*’ MATLAB function – for the annual morning peak net load demand hour of the MG operation, namely 10 a.m. July 21st. The corresponding deterministic values are as follows: irradiance = 161 W/m², temperature = 2.2 °C, wind speed = 4.1 m/s, streamflow = 4,129 L/s, load = 988 kWh, and wholesale price = \$0.11/kWh. Fig. 3 displays the convergence curve of the MFOA-optimized method applied to the deterministic case and the seven probabilistic cases, each addressing a year-long, hourly-basis reduced scenario vector. The figure reveals the adequacy of the optimizer's parameter settings and stopping criteria – a maximum of 200 iterations with 100 individuals – to yield a stable solution to the grid-tied MG sizing problem.

TABLE III. VALUE-PROBABILITY PAIRS FOR 10 A.M. JULY 21ST SCENARIOS

S	Prob.	Irrad. [W/m ²]	Temp. [°C]	Wind speed [m/s]	Flow [L/s]	Load [kWh]	Price [\$ /kWh]
1	0.230	149	1.9	4.4	4,125	1,027	0.13
2	0.197	171	2.4	3.9	3,962	972	0.11
3	0.163	159	2.0	4.0	4,077	1,013	0.09
4	0.155	151	1.9	3.6	4,574	904	0.08
5	0.119	175	2.4	2.9	4,117	1,098	0.11
6	0.092	189	3.8	4.7	3,716	821	0.07
7	0.044	117	0.8	6.8	4,428	1,110	0.16

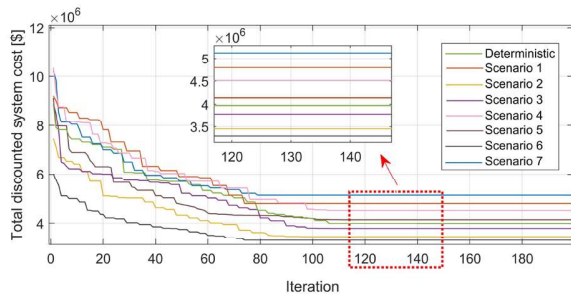


Figure 3. Convergence process of the MFOA embedded within the method.

Table IV provides a direct comparison of the deterministic and stochastic modelling results with the stochastic results detailing the middle-case (most likely case) and extreme-case (best-case and worst-case) scenarios – which are tailored to different uncertainty budgets. The table also compares the associated CPU usage times; the CPU execution time of the overall stochastic simulations is equal to the sum of the running times associated with the seven reduced year-long scenario vectors. Also, Fig. 4 shows the cumulative normal distribution function fit to the total discounted system cost data

with overlaid deterministic, expected (most likely), 5th percentile (best-case), and 95th percentile (worst-case) values.

TABLE IV. COMPARATIVE DETERMINISTIC AND PROBABILISTIC RESULTS

Output	Determin.	Simulation case		
		Stochastic		
		BC	ML	WC
Total NPC [\$m]	3.95	3.29	4.25	5.12
LCOE [\$ /kWh]	0.05	0.04	0.06	0.07
PV size [kW]	318	273	351	406
WT size [kW]	450	450	450	675
MHPP size [kW]	500	400	600	800
Battery size [kWh]	923	799	1,066	1,289
Inverter size [kW]	1,032	886	1,044	1,091
Trans. size [kVA]	389	371	417	433
Total annual net energy purchased [MWh]	-166.4	-191.3	-172.3	-218.3
Total annual net electricity exchange costs [\$k]	-9.98	-12.75	-11.3	-15.3
CPU usage time [s]	8,251	67,158		

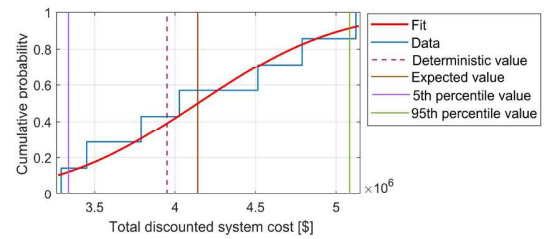


Figure 4. Fitting a cumulative normal distribution to the total NPC data.

Table IV and Fig. 4 are revealing in several ways, namely:

- The stochastic variant of the model is able to provide tailored decision support for effective investment planning of MGs, whilst accounting for various problem-inherent uncertainties – in accordance with the uncertainty budget of interest. Specifically, the most likely whole-life cost of the test-case MG indicates an 8% (equating to ~NZ\$0.3m) uncertainty cost premium above the deterministic cost estimates. Also, at the lower and upper extremes, which respectively represent the risk-seeking and risk-averse cases, the life-cycle cost of the system is found to be ~17% lower and ~30% higher than the deterministic case, respectively. The above asymmetry in the distribution of the investment cost data associated with different stochastic sub-models – where the mean of the population is greater than its median and therefore, the corresponding density function is positively-skewed – indicates that the additional cost incurred by a robust planning strategy is approximately double the savings of the corresponding opportunistic strategy with the same absolute value for the degree of conservatism.
- The percentage of the battery storage capacity to the total non-dispatchable power generation capacity in the cost-optimal solution set is found to be ~71%, ~76%, and ~68% in the best-case, most likely case, and worst-case scenarios, respectively. This observation suggests that the robust and opportunistic MG planning attitudes return mutually opposed solution sets in terms of the storage-to-generation ratio. Accordingly, at the current cost and technical performance of Li-ion battery storage for MG applications, the contribution of the storage capacity to narrowing the associated uncertainty bounds is found to be a concave-down quadratic function of the degree of conservatism – with the

vertex of the corresponding parabola located at the point associated with the risk-neutral (most likely) stochastic case.

- The overall running time of the stochastic model is 67,158 s, which is ~8.1 times higher than that of the deterministic model. More specifically, simulating the deterministic model for the seven year-long hourly reduced scenario vectors is responsible for a significant portion of the CPU time, taking 55,804 seconds of computational time. The remainder of the CPU usage time (11,354 s) was in clustering the hourly scenarios using the MILP-based scenario reduction algorithm, which takes less than 2 seconds of computational time to solve each hourly scenario reduction problem. While the stochastic model may be relatively computationally intensive, the decisions it is intended to support involve the planning of capital-intensive generation and storage assets.

VI. CONCLUSIONS

A computationally tractable model for meta-heuristic-based MG sizing that systematically and comprehensively accounts for probabilistic uncertainty associated with multiple input data – based on a heuristic scenario reduction algorithm – has been developed for the first time – towards improving the accuracy of the stochastic modelling results. A case study has been carried out to demonstrate the computational tractability of the proposed stochastic model for long-term MG investment planning in concurrently characterizing at least six sources of parametric uncertainty whilst retaining the statistical properties of the original scenario tree within an acceptable level. More specifically, the numeric results obtained from the application of the model to the test-case MG system populated for the town of Ohakune, New Zealand, have provided in-depth, accurate, and robust strategic capacity allocation and investment planning decision-making support in accordance with various uncertainty budgets. In particular, it is shown that the stochastic approach to MG designing incurs an (added) uncertainty treatment cost of ~8% (equating to ~NZ\$0.3m) and ~30% (~NZ\$1.17m) respectively in the most likely and worst-case scenarios compared to the deterministic MG investment planning results. In contrast, a strongly opportunistic designer who selects the least theoretically feasible infrastructure mix for the site of interest could expect a ~17% (~NZ\$0.66m) reduction in total discounted MG costs.

REFERENCES

- [1] S. Mohseni, A.C. Brent, D. Burmester, A. Chatterjee, "Stochastic Optimal Sizing of Micro-Grids Using the Moth-Flame Optimization Algorithm," in *Proc. 2019 IEEE Power & Energy Society General Meeting*, pp. 1–6.
- [2] S. Mohseni, A.C. Brent, D. Burmester, A. Chatterjee, "Optimal Sizing of an Islanded Micro-Grid Using Meta-Heuristic Optimization Algorithms Considering Demand-Side Management," in *Proc. 2018 Australasian Universities Power Engineering Conference*, pp. 1–6.
- [3] J.W. Whitefoot, "Optimal co-design of microgrids and electric vehicles: synergies, simplifications and the effects of uncertainty," Ph.D. Dissertation, Univ. Michigan, 2012.
- [4] G. Mavromatidis, K. Orehouing, J. Carmeliet, "A review of uncertainty characterisation approaches for the optimal design of distributed energy systems," *Renew. Sustain. Energy Rev.*, vol. 88, pp. 258–277, 2018.
- [5] J. Shin et al., "Operational planning and optimal sizing of microgrid considering multi-scale wind uncertainty," *Appl. Energy*, vol. 195, pp. 616–633, 2017.
- [6] G. Cardoso et al., "Optimal investment and scheduling of distributed energy resources with uncertainty in electric vehicle driving schedules," *Energy*, vol. 64, pp. 17–30, 2014.
- [7] S. Mohseni, A.C. Brent, D. Burmester, W.N. Browne, "Lévy-flight moth-flame optimisation algorithm-based micro-grid equipment sizing: An integrated investment and operational planning approach," *Energy AI*, vol. 3, p. 100047, 2021.
- [8] A. Hussain et al., "Optimal siting and sizing of tri-generation equipment for developing an autonomous community microgrid considering uncertainties," *Sustain. Cities Soc.*, vol. 32, pp. 318–330, 2017.
- [9] S.A. Mansouri, A. Ahmarinejad, M.S. Javadi, J.P.S. Catalão, "Two-stage stochastic framework for energy hubs planning considering demand response programs," *Energy*, vol. 206, p. 118124, 2020.
- [10] D.R. Prathapaneni, K.P. Detroja, "An integrated framework for optimal planning and operation schedule of microgrid under uncertainty," *Sustain. Energy Grids Networks*, vol. 19, p. 100232, 2019.
- [11] H. Baghaee, M. Mirsalim, G. Gharehpetian, H. Talebi, "Reliability/cost-based multi-objective Pareto optimal design of stand-alone wind/PV/FC generation microgrid system," *Energy*, vol. 115, pp. 1022–1041, 2016.
- [12] A. Masoumi, S. Ghassem-Zadeh, S. Hosseini, B. Ghavidel, "Application of neural network and weighted improved PSO for uncertainty modeling and optimal allocating of renewable energies along with battery energy storage," *Appl. Soft Computing*, vol. 88, p. 105979, 2020.
- [13] V. Amir, M. Azimian, "Dynamic Multi-Carrier Microgrid Deployment Under Uncertainty," *Appl. Energy*, vol. 260, p. 114293, 2020.
- [14] B. Li, R. Roche, "Microgrid sizing with combined evolutionary algorithm and MILP unit commitment," *Appl. Energy*, vol. 188, pp. 547–562, 2017.
- [15] S. Mohseni, A.C. Brent, D. Burmester, "A Sustainable Energy Investment Planning Model Based on the Micro-Grid Concept Using Recent Metaheuristic Optimization Algorithms," in *Proc. 2019 IEEE Congress on Evolutionary Computation*, pp. 219–226.
- [16] S. Sun et al., "Effects of time resolution on finances and self-consumption when modeling domestic PV-battery systems," *Energy Reports*, vol. 6, pp. 157–165, 2020.
- [17] S. Mohseni, A.C. Brent, D. Burmester, "Community Resilience-Oriented Optimal Micro-Grid Capacity Expansion Planning: The Case of Totarabank Eco-Village, New Zealand," *Energies*, vol. 13, no. 15, p. 3970, 2020.
- [18] S. Mohseni, A.C. Brent, S. Kelly, "A hierarchical, market-based, non-cooperative game-theoretic approach to projecting flexible demand-side resources: Towards more realistic demand response-integrated, long-term energy planning models," in *Proc. 2020 17th International Conference on the European Energy Market*, pp. 1–6.
- [19] S. Mirjalili, "Moth-flame optimization algorithm: A novel nature-inspired heuristic paradigm," *Knowledge-Based Syst.*, vol. 89, pp. 228–249, 2015.
- [20] S. Mohseni, A.C. Brent, D. Burmester, W. Browne, "A Game-Theoretic Approach to Model Interruptible Loads: Application to Micro-Grid Planning," in *Proc. 2020 IEEE Power & Energy Society General Meeting*, pp. 1–5.
- [21] S. Mohseni, A.C. Brent, D. Burmester, "Off-Grid Multi-Carrier Microgrid Design Optimisation: The Case of Rakiura–Stewart Island, Aotearoa–New Zealand," *Energies*, vol. 14, no. 20, p. 6522, 2021.
- [22] R. Karupiah, M. Martín, I. E. Grossmann, "A simple heuristic for reducing the number of scenarios in two-stage stochastic programming," *Comput. Chem. Eng.*, vol. 34, no. 8, pp. 1246–1255, 2010.
- [23] S. Mohseni, A.C. Brent, S. Kelly, D. Burmester, W. Browne, "Modelling utility-aggregator-customer interactions in interruptible load programmes using non-cooperative game theory," *Int. J. Electr. Power Energy Syst.*, vol. 133, p. 107183, 2021.
- [24] CliFlo: New Zealand's national climate database. [Online]. Available: <http://cliflo.niwa.co.nz/> [Retrieved: 9-Jan.-2021].
- [25] B. Anderson, D. Evers, R. Ford, D.G. Ocampo, R. Peniamina, J. Stephenson, K. Suomalainen, L. Wilcocks, M. Jack. New Zealand GREEN grid household electricity demand study 2014–2018. Colchester, Essex: UK Data Service [Retrieved: 9-Jan.-2021].
- [26] The Electricity Market Information. The New Zealand electricity authority's wholesale database. [Online]. Available: <https://www.emi.ca.govt.nz/Wholesale/Reports/> [Retrieved: 9-Jan.-2021].